Geostatistical mapping of the depth to the bottom of magnetic sources and heat flow estimations in Mexico

Juan Luis Carrillo-de la Cruz [a,b], Rosa María Prol-Ledesma [b], Gerald Gabriel [c,d,*]

[a] *Posgrado en Ciencias de la Tierra, Instituto de Geofísica, Universidad Nacional Autónoma de México, Circuito interior s/n, Coyoacán, 04510 Ciudad de México, México*
[b] *Instituto de Geofísica, Universidad Nacional Autónoma de México, Circuito interior s/n, Coyoacán, 04510 Ciudad de México, México*
[c] *Leibniz Institute for Applied Geophysics, Stilleweg 2, 30655 Hannover, Germany*
[d] *Institut für Geologie, Leibniz Universität Hannover, Callinstraße 30, 30167 Hannover, Germany*

ARTICLE INFO

ABSTRACT

The depth to the bottom of magnetic sources (DBMS) is widely used as a proxy for crustal thermal structures. In this study, the DBMS is calculated using the spectral analysis of aeromagnetic data for the whole territory of Mexico. By assuming the DBMS to be related to the Curie point depth, the heat flow distribution is estimated. The DBMS and heat flow maps were constructed using geostatistical simulations to quantitatively determine standard deviation as uncertainty. The results show a good agreement with the complex geologic and tectonic setting in Mexico. Small DBMS values (high heat flow) as expected appear in areas where recent volcanism occurs and at seafloor spreading zones. In contrast, large values are present in tectonically stable zones.

1. Introduction

Different geophysical properties are studied to understand the Earth's dynamics, among them the thermal state of the crust. However, a lack of direct temperature measurements at depth hinders the knowledge of the Earth's crust thermal state. Therefore, other approaches to estimate the temperature are commonly used to evaluate the thermal regime at large depths, e.g., chemical geothermometers or Curie point depth estimations.

The estimation of the depth to the bottom of magnetic sources (DBMS), commonly used as a proxy of the Curie point depth (CPD), is a widely used approach for regional studies of the thermal structure of the Earth, when surface heat flow data are not available (Blakely, 1988; Bouligand et al., 2009; Ross et al., 2006; Tanaka et al., 1999).

In this study, the DBMS was calculated by the spectral analysis of aeromagnetic anomalies, using the modified centroid method with variable window size depending on the regional geological setting, and the construction of the DBMS map for Mexico was accomplished using geostatistical modeling, this way the uncertainties could be quantitatively determined. The resulting DBMS values were compared with surface heat flow (boreholes and seafloor) measurements to identify the relation between the borehole data and the DBMS calculation.

2. Materials and methods

To derive the depth to the bottom of magnetic sources (DBMS), the long wavelength part of the magnetic anomalies is studied in squared windows. For this reason, regional data is required that cover a sufficiently large area. Aeromagnetic data compilations or satellite magnetic data are the common datasets used for this purpose.

2.1. Aeromagnetic data

In this work, the North American Magnetic Anomaly Map (NAMAG, 2002) was used (Fig. 1). The NAMAG data is provided as 1-km grid, referred to the Decade of North American Geology projection (DNAG). For the compilation of the map, every data set was field continued to the common reference level of 305 m above terrain. Anomalies were calculated by subtracting the Definitive Geomagnetic Reference Field (DGRF), updated to every survey date, from the total magnetic field. This dataset was already used by several authors to calculate the DBMS, either for other North American countries or some isolated parts of Mexico, e.g., Bouligand et al. (2009), Campos-Enriquez et al. (2019), Carrillo-de la Cruz et al. (2020a, 2020b), Manea and Manea (2011), and Wang and Li (2015).

---

* Corresponding author.
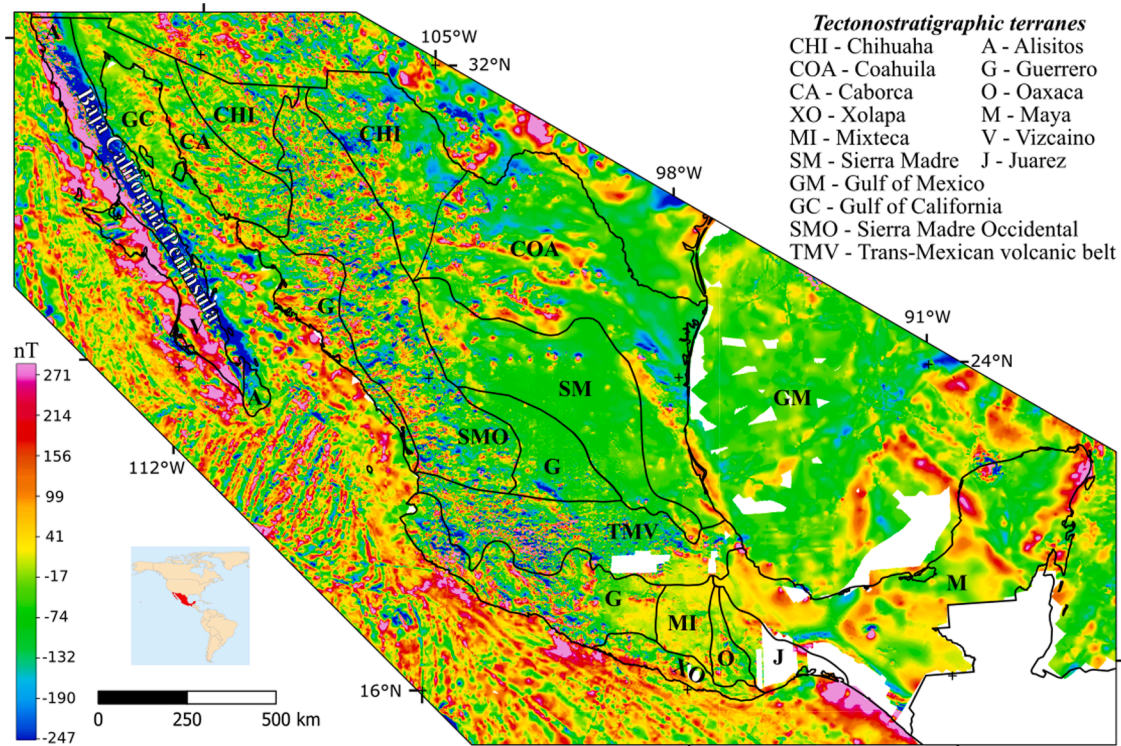*E-mail address:* gerald.gabriel@leibniz-liag.de (G. Gabriel).

Fig. 1. Tectonostratigraphic terranes (modified after Campa and Coney, 1983) and the relevant part of the Magnetic Anomaly Map of North America (data from the North American Magnetic Anomaly Group NAMAG, 2002). White areas represent lack of magnetic data.
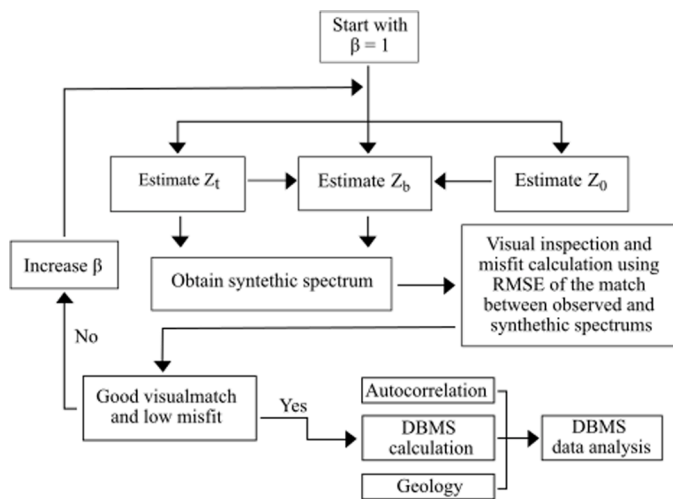

Fig. 2. Flowchart for the DBMS calculation in the present study (modified from Salem et al., 2014; Martos et al., 2017).

2.2. Depth to the bottom of magnetic sources estimations

Several methods are available for the DBMS estimation. Recent studies suggest that the fractal magnetization model methods are the most reliable (Bansal et al., 2011; Bouligand et al., 2009; Carrillo-de la Cruz et al., 2020a; Kumar et al., 2020; Li et al., 2013). For this research, the DBMS (z_b) calculation for Mexico is carried out by using the modified centroid method (Carrillo-de la Cruz et al., 2020b; Li et al., 2013) because this method considers a fractal magnetization model. DBMS was calculated using an early version of MAGCPD program (Carrillo-de la Cruz et al., 2020b).

To estimate the depth to the top (z_t) and the centroid (z_0) of the magnetic sources, it is necessary to analyze the slope of a straight-line that fits the middle and low wavenumber parts of the amplitude spectrum and the scaled amplitude spectrum, respectively. Subsequently, the DBMS (z_b) is estimated by using Eq. (1).

$$z_b = 2z_0 - z_t \tag{1}$$

From an iterative forward modeling, z_t, z_0 and z_b are calculated by using different values of the fractal parameter (β) and wavenumber ranges of the spectra. The fractal parameter is related to the 3-D power spectrum ϕ_m of the magnetization by $\phi_m(k_x, k_y, k_z) \propto k^{-\beta}$. To get reliable DBMS results, the root-mean square error (RMSE), and the visual inspection of the similarity between the synthetic spectra (obtained by the forward modeling of the results) and the observed spectra, alongside with the autocorrelation function and the geology, are essential (Fig. 2). The method uncertainty is calculated by the approach of Martos et al. (2017) and depends on the standard deviation of the radial power spectrum (see Supplementary material).

To apply this methodology, it is mandatory to calculate the radially averaged amplitude spectrum from magnetic data within square windows. The suitable window size is still a matter of scientific discussion. For this reason, the windows size used to calculate the radially averaged amplitude spectrum is in general variable, i.e. between five to ten times the expected DBMS (Kumar et al., 2020; Ravat et al., 2007). The suitable size of every window depends on geology and the tectonic setting that affects the thermal state of the crust. Due to the complexity of the geological framework of Mexico, the present study considers the tectonostratigraphic terranes after Campa and Coney (1983) as the main generalization of the geological framework, because these terranes are closely related to the anomalies of the Earth's total magnetic field in Mexico (Fig. 1).

2.3. Heat flow estimations

DBMS is commonly used as a proxy for the Curie point depth that defines the depth where the crustal temperature exceeds the Curie
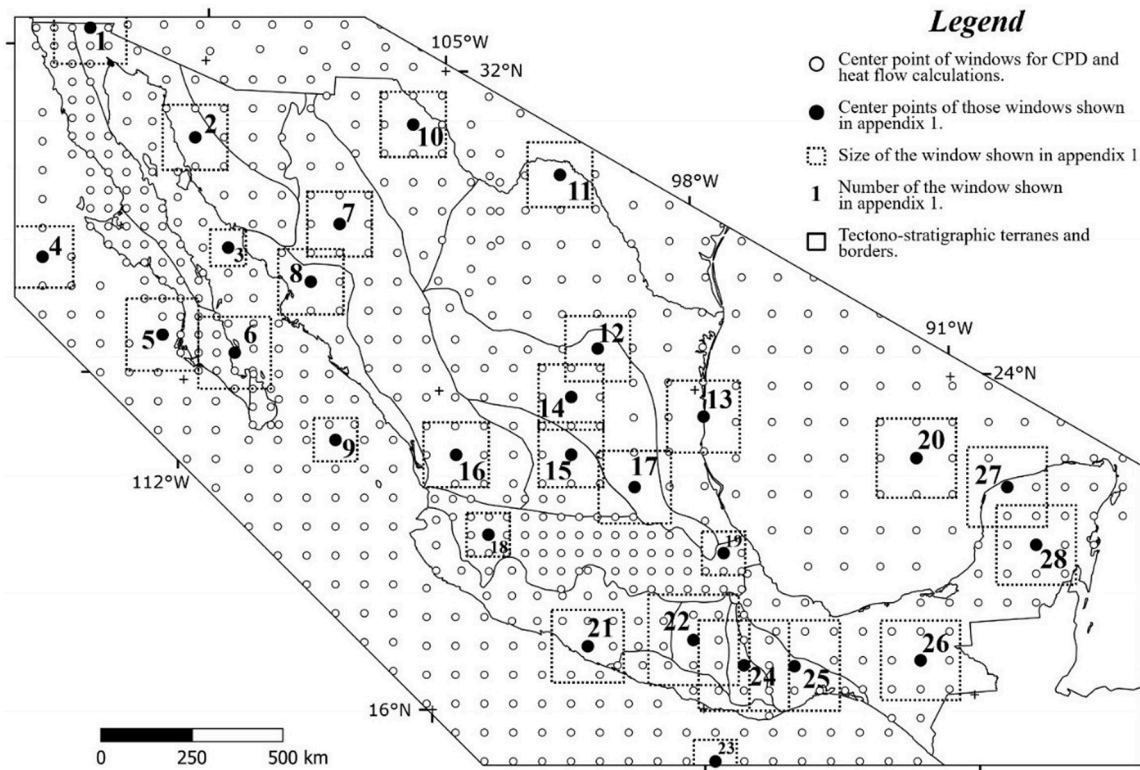
Fig. 3. Representative window size depending on the tectono-stratigraphic terranes presented in Fig. 1. Dots denote window centers and numbers indicate those windows that are part of the Supplementary material (Figure S1).

temperature of the magnetic minerals and, thus, the rocks become paramagnetic. The accepted convention is to use the Curie temperature of magnetite, which is 580 °C, as the reference Curie temperature.

The heat flow calculations in this study use a 1-D (vertical) steady-state heat conduction equation with heat production decreasing exponentially with depth (Turcotte and Schubert, 2002):

$$\lambda \frac{\partial^2 T(z)}{\partial z^2} = -H_0 e^{-(z-z_s)/h_r} \tag{2}$$

where λ is the thermal conductivity, T temperature, z_s Earth surface, z depth, H_0 heat production at the surface z_s, and h_r a scaling length for H_0 that decreases with depth.

By integrating Eq. (2) and applying the boundary conditions $z = z_b$ (CPD), $z_s = 0$ (surface), the heat flow becomes:

$$q_s = \frac{\lambda(T_c - T_0)}{z_b} + H_0 h_r - \frac{H_0 h_r^2}{z_b}\left(1 - e^{(-z_b/h_r)}\right) \tag{3}$$

with T_c being the Curie temperature at depth z_b and T_0 the temperature at the surface (Martos et al., 2017).

2.4. Stochastic simulations

The process of simulated alternative, equally probable, joint realization of the random variables in a random function model is called stochastic simulation (Deutsch and Journel, 1998). These stochastic simulations attempt to replicate reality using a model, which is the appropriate approach when constructing a map. The Sequential Gaussian Simulation (SGS) is used in this research to draw maps and assess the spatial variability of the DBMS and heat flow. SGS produces more accurate maps than kriging because it solves problems caused by the kriging method in terms of overestimated high values or underestimated low values. Details of the SGS algorithm are described by Cardellini et al. (2003), Deutsch and Journel (1998), and Pyrcz and

Deutsch (2014).

For the application of the SGS it is important to have a Gaussian distribution of the data. However, most data that describe geological processes do not fit this distribution; hence, data transformations are necessary. For this reason, the SGS algorithm follows these generalized steps (Pyrcz and Deutsch, 2014):

- Selection of the grid system and the coordinate system for the study area.
- Data input in the grid system.
- Normal Score Transformation, that is, the original data needs to be transformed into a normal space (Gaussian distribution).
- Calculation of the normal score semivariogram.
- Construction of the conditional distribution using kriging.
- Calculation of a simulated value using the conditional distribution.
- Simulated value input in the grid.
- Verification of all locations in the grid randomly.
- Validation of the simulated data using the histogram $N(0, 1)$ and the normal score semivariogram.
- Transformation of the data to the original Cumulative Distribution Function (CDF).
- Recalculation of the simulation using random numbers.

The results are shown as expected value models (also called e-type models) and conditional variance models pixel-by-pixel.
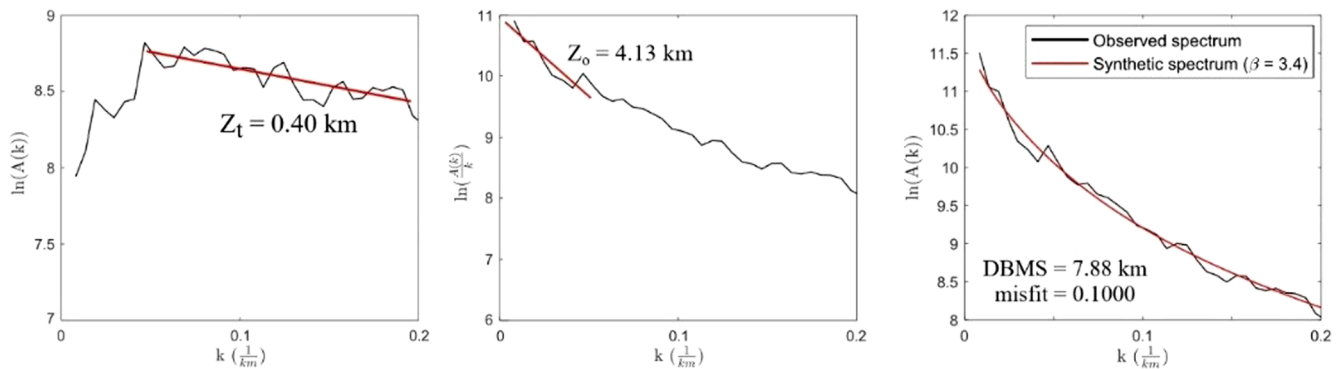
3. Applications

The methodology to construct the regional DBMS and heat flow maps of the continental and the marine region of Mexico includes the spectral analysis of aeromagnetic data, heat flow calculation and the statistical analysis of the results using the Sequential Gaussian Simulation.
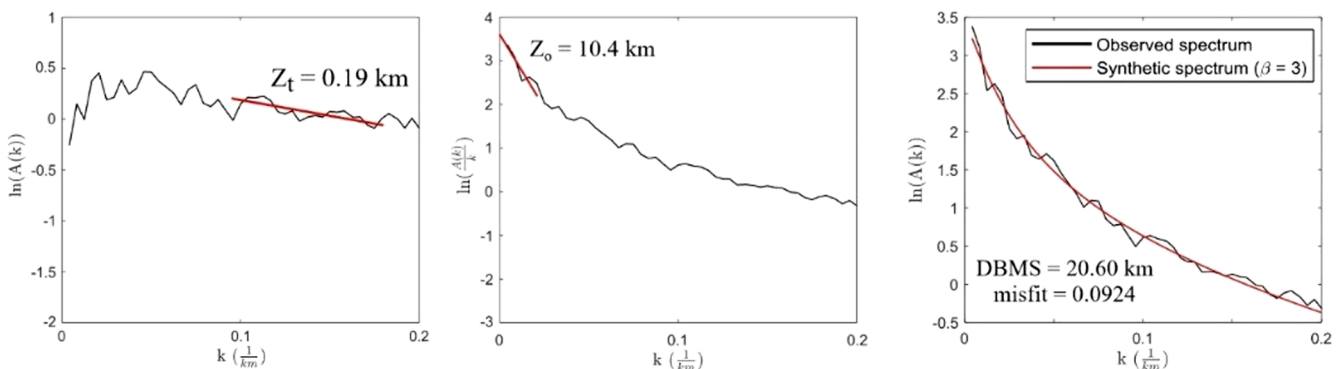
Window 5
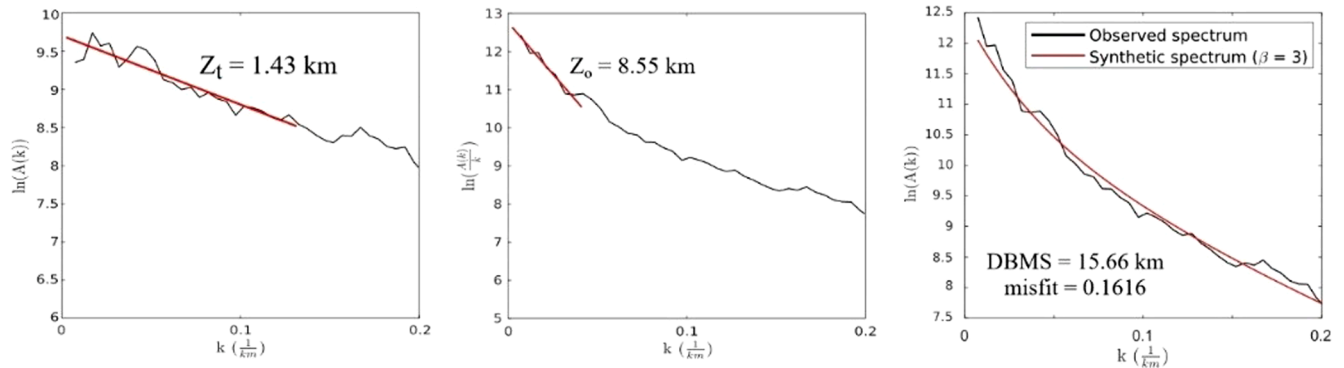
Window 16

Window 24

Fig. 4. Examples of windows located in different tectonostratigraphic terranes, showing the wavenumber ranges used to calculate the DBMS and the adjust between the synthetic and the observed spectra in the forward modeling; z_t top of the magnetized layer, z_0 centroid depth, β fractal parameter.

3.1. Depth to the bottom of magnetic source calculation

The calculation of the DBMS involves several subsequent steps (see Supplementary material and Fig. 2). The size of the used windows is variable, depending on the geological environment. In areas where the CPD is expected to be shallow (e.g., volcanic areas or ocean spreading zones), a small square window size in the order of 100 km - 150 km is used, whereas in zones with an expected large CPD (e.g., the tectonically stable zones) a larger window size in the order of 200 km or more is used. The window size must be large enough to reveal the magnetic signatures caused by the deepest magnetic sources for each geological province. Fig. 3 shows Mexico's tectonostratigraphic terranes, the window size for the data analysis, and the number of the windows presented as representative examples in Figure S1 at Supplementary material.

The definition of the wavenumber ranges used to calculate the slopes in the amplitude spectra and the scaled amplitude spectra vary depending on the geological setting. Additionally, the complete homogeneity of each terrain in terms of its magnetization is not a realistic assumption. Consequently, the wavenumber ranges change slightly in the various calculations to ensure a reasonable adjustment of the synthetic spectrum to the original spectrum during the forward modeling. Figs. 4 and S1 present examples for the different slopes used.

The autocorrelation function in windows 5 and 6 (Figs. 5a and S1) reveal a NW-SW oriented ellipse, related to a strong trend caused by the Peninsular Range Batholith. Similarly, windows 23, 3, and 4 (Figs. 5b and S1) show a trend related to the ocean floor spreading magnetic strip geometry. In addition, an apparent data trend in window 13 (Fig. 5c) is related to the NW-SE striking high-amplitude anomaly caused by
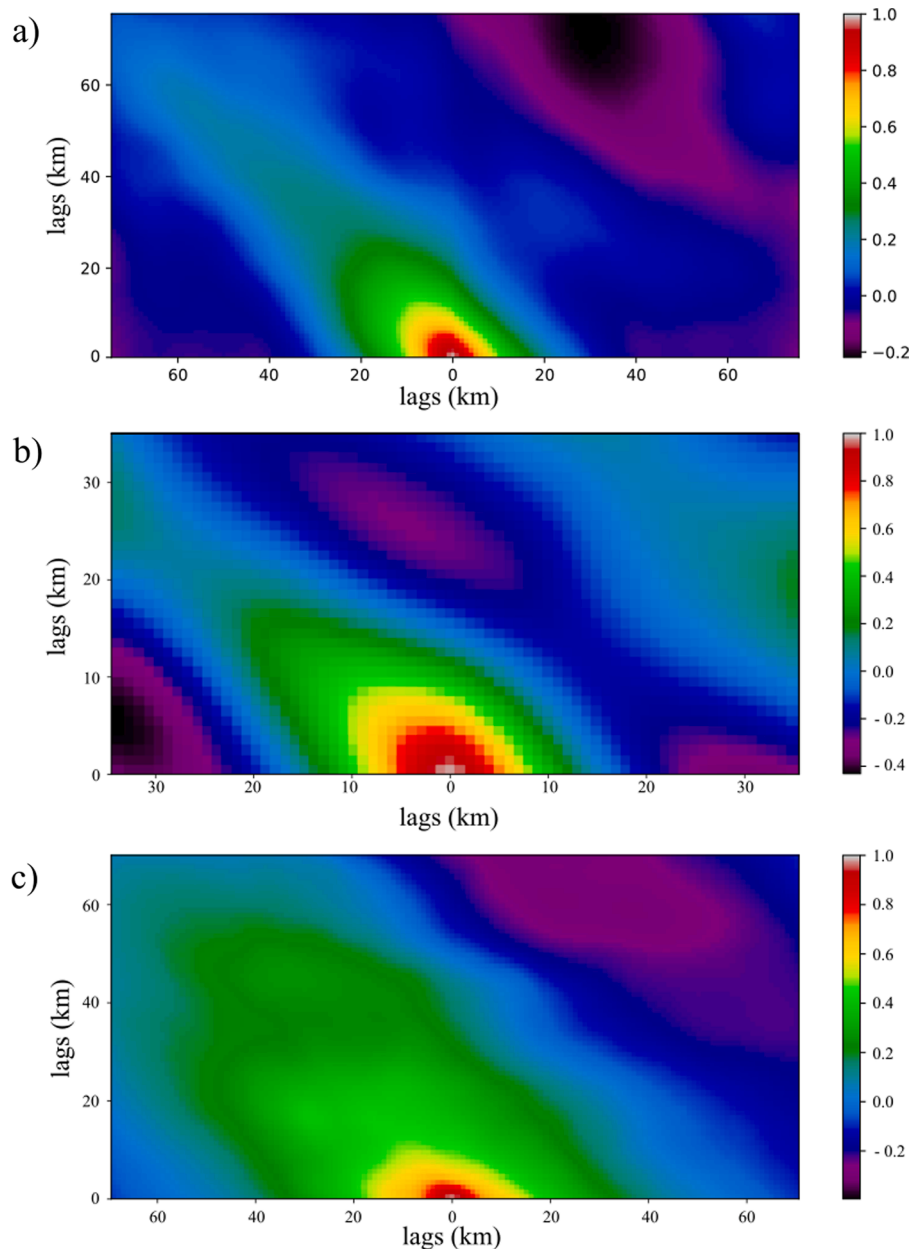
Fig. 5. Autocorrelation function: examples for a) window 5, b) window 23, and c) window 13.

basement structures of the Sierra Madre.

3.2. Heat flow estimations using the DBMS

The heat flow (Eq. (3)) is calculated using thermal parameter values as summarized in Table S2, considering the DBMS (z_b) as the CPD, taking the Curie temperature of magnetite (580 °C), and a constant value for the scaling length h_r of 10 km (see Turcotte and Schubert, 2002). In Table S2, the values of thermal conductivity and heat generation rate are an average value for the representative rock types for each tectonostratigraphic terrane. To calculate the heat flow, it is necessary to subtract the reference height of the airborne data (305 m) from the DBMS results, because Eq. (3) is referred to surface.

3.3. Sequential gaussian simulation (SGS) application

The use of the geostatistical libraries (or GSLIB), published by Deutsch and Journel (1998), was essential for the realization of this study. The simulation, using SGS, is applied using the GSLIB module *sgsim*. Following the theory behind *sgsim*, the data need to be analyzed statistically before performing each simulation. By using the semivariogram, a regional trend was found in the data (Fig. S2 at Supplementary material). For this reason, the data need to be detrended and simulation is applied to the data residuals. From the one hundred simulations, the DBMS and heat flow map result, and by comparing the simulation models with the original data (Figs. S3 and S4 at Supplementary material), the simulations reproduce the original data with small fluctuations (see Supplementary material).

4. Results

Based on the spectral analysis of aeromagnetic anomalies and the application of the modified centroid method, DBMS and heat flow values were calculated for 722 windows of variable size. These values were analyzed using geostatistics to provide a map and examine the spatial patterns of the calculated DBMS and heat flow as well as their rela-
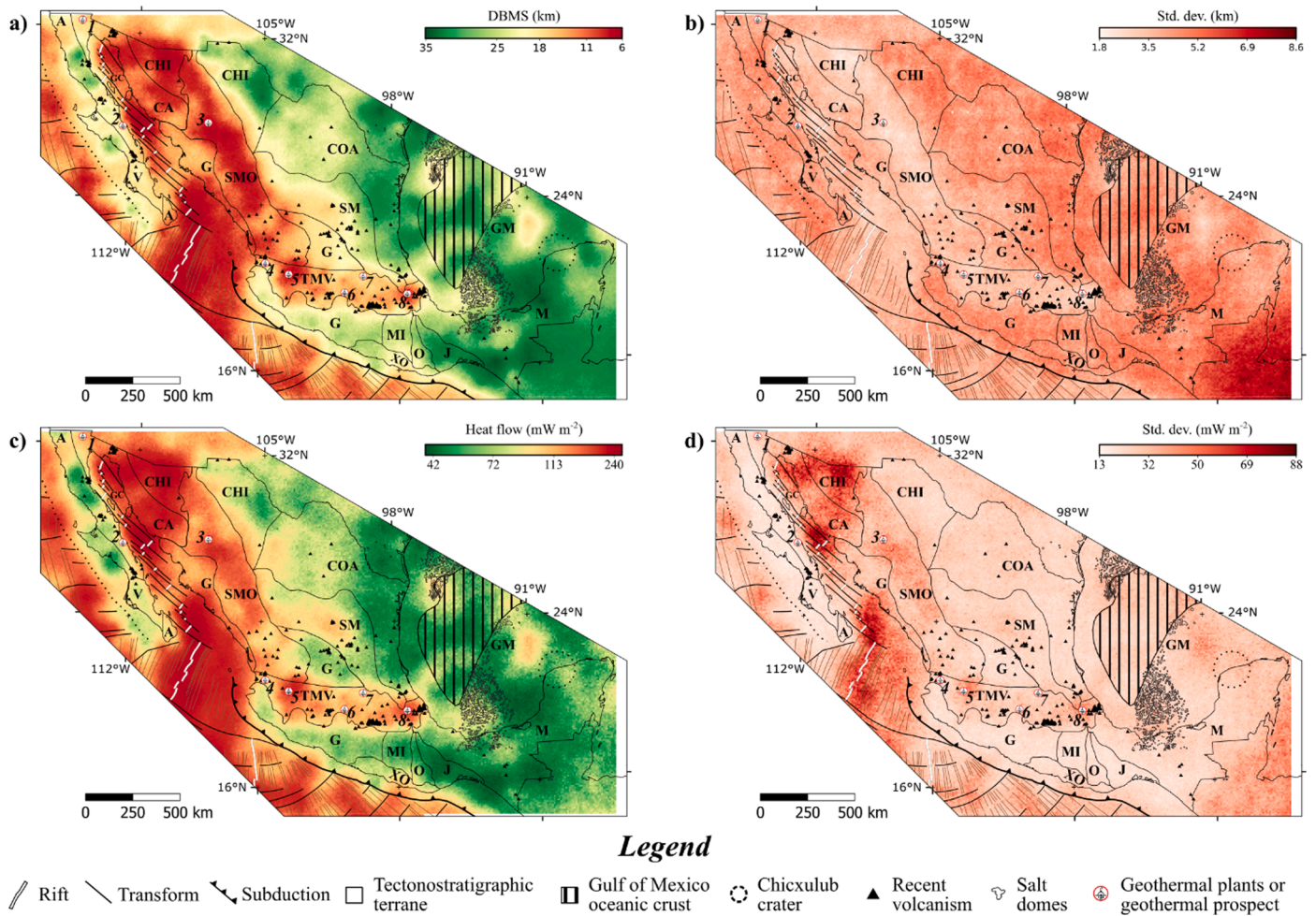
Fig. 6. a) DBMS e-type map, b) DBMS standard deviation map, c) heat flow e-type map, and d) heat flow standard deviation map with the main tectonic features. Tectonic features from the Tectonic Map of Mexico 2013 (Padilla y Sánchez et al., 2013). Geothermal plants and prospective geothermal areas: 1) Cerro Prieto, 2) Las Tres Vírgenes, 3) Piedras de Lumbre-Maguarichic, 4) Domo San Pedro, 5) La Primavera-Cerritos Colorados, 6) Los Azufres, 7) Pathé, and 8) Los Humeros. Recent volcanoes (< 3Ma) from Prol-Ledesma et al. (2018). Abbreviations from Fig. 1.

Table 1
Statistics for the entire study area.

Simulation	Original data			Simulation data		
	Mean	Std. dev.	5th – 95th percentiles	Mean	Std. dev.	5th – 95th percentiles
DBMS (km)	17.1	7.7	7.3 – 32.1	17.0	6.0	9.0 – 27.1
heat flow (mW m^{-2})	98.6	44.0	49.1 – 176.2	97.0	33.8	56.3 – 162.9

tionship to regional tectonics. Simulation results are presented as maps of the e-type DBMS and heat flow (Fig. 6). From the e-type models, the average heat flow of the continental part of Mexico is 85 ± 27 mW m^{-2}, exceeding the global continental average of 64.7 mW m^{-2} (Davies, 2013) by more than 30%. In contrast, the average values for the oceanic part of Mexico are 103 ± 39 mW m^{-2}, an average value slightly above the global oceanic average of 95.9 mW m^{-2} (Davies, 2013). Table 1 shows the statistics of the entire study area and reveals that the fluctuations between the 722 windows and the simulation results are small.

The results show that the variations of DBMS and heat flow are related to the main tectonic features, e.g., the shallower DBMS and the highest heat flow occur in spreading zones and regions of recent volcanic activity.

5. Discussion

The wavenumber ranges used to obtain z_t and z_0 depend on the characteristics of the slopes of the spectra and the adjustment between the observed amplitude spectra and the synthetic spectra. These considerations are different for every geological terrane, and frequently in the same terrane the wavenumber range differs between two analyzed windows. The pre-analysis of the spectra in terms of the autocorrelation function of the aeromagnetic data helps to find trends in the data. Some geological structures cause significant trends in the magnetic data, e.g., the trend related to the Peninsular Range Batholith (Baja California peninsula) and the ocean spreading zones. In both cases, the DBMS result could be biased and does not totally represent the CPD.

Active tectonic zones and the presence of recent volcanism are related with small DBMS and high heat flow values. The main volcanic terranes (Sierra Madre Occidental and Trans-Mexican Volcanic belt terranes) show a direct correlation between small DBMS (and high heat flow values) and recent volcanic activity. At Sierra Madre Occidental terrane, the thermal anomalies could be related with volcanism and the high content of radioactive elements (U, Th, and K) that contributes more than 30% to the surface heat flow (Smith et al., 1979).

For the Gulf of California, shallow DBMS is related with the rifting process, and the heat flow values derived from the DBMS are above 200 mW m^{-2}. At the center of the Baja California peninsula (Alisitos and Vizcaino terranes), the deepest DBMS values (> 20 km) are possibly
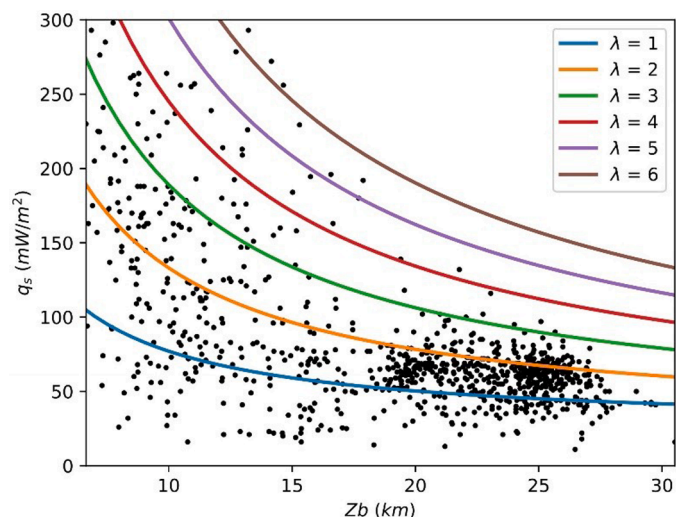
Fig. 7. Scatterplots of heat flow from boreholes and seafloor vs. DBMS ($r^2 =$ 0.32). Colored lines indicate the relations when applying Eq. (3) for different thermal conductivities (in $\frac{W}{m\,K}$), 580 °C as the Curie temperature, 20 °C as the surface temperature, 2.5 $\frac{\mu W}{m^3}$ as heat generation rate, and h_r of 10 km. Sources: heat flow data from Prol-Ledesma et al. (2018) and SMU Node of National Geothermal Data (SMU, 2020). Boreholes and seafloor heat flow data distribution is presented in figure S5 in Supplementary material.

related to the presence of the Farallon-remnant fossil slab (Wang et al., 2013).

South of the Trans-Mexican Volcanic belt terrane, at the Guerrero, Mixteca, Oaxaca, Juarez and Xolapa terranes, the DBMS values are larger than 18 km (< 75 mW m^{-2}), showing a pattern similar to that obtained by Okubo et al. (1989) for a subduction zone, where the heat flow next to the volcanic front starts to decrease. This decrease in the heat flow values is produced by the flat-slab regime in a temperature decrease caused by the plate cooling, as was also obtained in previous research (Manea and Manea, 2011).

Our DBMS results for the Gulf of California are similar to the results presented by Campos-Enríquez et al. (2019); nevertheless, our results yield deeper values for DBMS in some areas of the Baja California peninsula. Alternatively, at the Guerrero, Mixteca, Oaxaca, Juarez and Xolapa terranes, our results are in the range of $\sim$ 20 to 30 km, that are consistently deeper than those presented by Manea and Manea (2011) ($\sim$ 16 to 24 km). In both cases, the difference between DBMS calculations could be related with the methodology and the wavenumber range employed. For example, Manea and Manea (2011) used a constant wavenumber range, while in our study it is variable depending on the geological framework. Campos et al. (2019) do not present an error estimation map, while Manea and Manea (2011) present only the map for the z_0 error estimation. The conditional standard deviation derived from Sequential Gaussian Simulations (Fig. 5b and 5d) defines the map uncertainty; it is worth to mention that the uncertainty maps for DBMS and heat flow have not been presented by previous studies of DBMS calculations from aeromagnetic data in Mexico.

The use of geostatistical simulations in DBMS and heat flow mapping allows ascertaining the statistical variability of every estimated value in the map. The advantage of using geostatistical simulations in comparison to other interpolation methods (e.g., kriging) is the uncertainty quantification as standard deviation maps.

The heat transfer mechanism is the most important parameter in the calculation of the heat flow. Guerrero-Martínez et al. (2020) used the DBMS as a boundary condition to simulate heat transfer in the Acoculco caldera, located at the Trans-Mexican Volcanic Belt. Their results show that local heat sources would not be evident in a regional model, i.e., on the scale on which the DBMS is calculated. Similarly, the intense

convection in the Cerro Prieto hydrothermal system that promotes a more efficient heat transport and the DBMS values calculated for Cerro Prieto ($\sim$15 km) do not reproduce the 79–90 °C/km geothermal gradient (expected DBMS $\sim$7 km) measured from wells (Prol-Ledesma et al., 2016). The convection effects in the geothermal gradient are not expressed in the results of heat flow estimation using DBMS/CPD, as observed in other DBMS/CPD calculations for Cerro Prieto (Campos-Enríquez et al., 2019).

Heat flow calculations based on DBMS values were compared with heat flow data from boreholes and seafloor data (Figure S5 in Supplementary material); the theoretical curves in Fig. 7 result from Eq. (3). The in-situ data have a wide scattering, showing a similar trend than those presented in other studies (Li et al., 2010, 2013; Wang and Li, 2015). Fig. 7 shows that most data cluster on theorical curves that corresponds to thermal conductivities between 1 and 3 $\frac{W}{m\,K}$. The data scattering in relation with the presented theoretical curves is consistent with changes of the thermal parameters at depth (Curie temperature, thermal conductivity, and/or heat generation rate) or different heat transfer mechanisms.

6. Conclusions

The depths to the bottom of the magnetic sources (DBMS) of Mexico were calculated by using a combination of the modified centroid method and forward modeling of the radially averaged amplitude spectrum. Heat flow is estimated based on the DBMS derived from magnetic anomaly data. Finally, the DBMS and heat flow maps of Mexico were generated by applying for the first-time geostatistical simulations. The most important conclusions derived with respect to the methodology and geological interpretations are:

- The autocorrelation function characteristics turned out to be an important tool to analyze trends in magnetic data that could affect the DBMS calculations.
- The lower and middle wavenumber range used to calculate the top and centroid of the magnetic sources are selected depending on the detectable slopes in the spectra; the spectra change, depending on the geological setting. The selection of wavenumber ranges affects the forward modeling.
- Geostatistical simulations, firstly applied in this study in the context of the DBMS, provide a robust quantification of the spatial patterns and the spatial uncertainties.
- The effective thermal conductivity of Mexico is between 1 and 3 $\frac{W}{m\,K}$, and the presence of different heat transfer mechanism at local scale affect the relation between DBMS and heat flow from borehole and seafloor data (Fig. 7).
- For hydrothermal reservoirs, the DBMS values differ significantly from the borehole data due to heat being transferred convectively as well as conductively in the hydrothermal reservoirs. This is shown for two active geothermal fields (Cerro Prieto and Acoculco).
- For this study, the estimated average heat flow value for the continental part of Mexico is significantly higher than the global continental average, whereas the averaged estimated heat flow value for the oceanic part of the study area is only slightly higher than the global average. This is interpreted as a consequence of two effects: active sea floor spreading in extensive areas in the western Pacific areas nearby Mexico and the low heat flow and large DBMS in the Gulf of Mexico.

CRediT authorship contribution statement

Juan Luis Carrillo-de la Cruz: Methodology, Formal analysis, Writing – original draft. **Rosa María Prol-Ledesma:** Conceptualization, Supervision, Writing – review & editing. **Gerald Gabriel:** Supervision, Methodology, Writing – review & editing.

Declaration of Competing Interest

The authors declare that they have no known competing financial interests or personal relationships that could have appeared to influence the work reported in this paper.

Supplementary materials

Supplementary material associated with this article can be found, in the online version, at doi:10.1016/j.geothermics.2021.102225.

References

Bansal, A.R., Gabriel, G., Dimri, V.P., Krawczyk, C.M., 2011. Estimation of depth to the bottom of magnetic sources by a modified centroid method for fractal distribution of sources: an application to aeromagnetic data in Germany. Geophysics 76 (3), L11–L22. https://doi.org/10.1190/1.3560017.

Blakely, R.J., 1988. Curie temperature isotherm analysis and tectonic implications of aeromagnetic data from Nevada. J. Geophys. Res. Solid Earth 93 (B10), 11817–11832. https://doi.org/10.1029/JB093iB10p11817.

Bouligand, C., Glen, J.M.G., Blakely, R.J., 2009. Mapping Curie temperature depth in the western United States with a fractal model for crustal magnetization. J. Geophys. Res. 114, B11104. https://doi.org/10.1029/2009jb006494.

Campa, M.F., Coney, P.J., 1983. Tectono-stratigraphic terranes and mineral resource distributions in Mexico. Can. J. Earth Sci. 20, 1040–1051. https://doi.org/10.1139/e83-094.

Campos-Enríquez, O.C., Espinoza-Cardeña, J.M., Oskum, O., 2019. Subduction control on the Curie isotherm around the Pacific-North America plate boundary in northwestern Mexico (Gulf of California). Preliminary results. J. Volcanol. Geothermal Res. 375, 1–17. https://doi.org/10.1016/j.jvolgeores.2019.03.005.

Cardellini, C., Chiodini, G., Frondini, F., 2003. Application of stochastic simulation to CO2 flux from soil: mapping and quantification of gas release. J. Geophys. Res. 18 (B9), 2425. https://doi.org/10.1029/2002JB002165.

Carrillo-de la Cruz, J.L., Prol-Ledesma, R.M., Gómez-Rodríguez, D., Rodríguez-Díaz, A. A., 2020a. Analysis of the relation between bottom hole temperature data and Curie temperature depth to calculate geothermal gradient and heat flow in Coahuila. Mexico. Tectonophysics 780, 228397. https://doi.org/10.1016/j.tecto.2020.228397.

Carrillo-de la Cruz, J.L., Prol-Ledesma, R.M., Velázquez-Sánchez, P., Gómez-Rodríguez, D., 2020b. MAGCPD: a MATLAB-based GUI to calculate the Curie point-depth involving the spectral analysis of aeromagnetic data. Earth Sci. Inf. https://doi.org/10.1007/s12145-020-00525-x.

Davies, J.H., 2013. Global map of solid Earth surface heat flow. Geochem. Geophys. Geosyst. 14 (10), 4608–4622. https://doi.org/10.1002/ggge.20271.

Deutsch, C.V., Journel, A.G., 1998. GSLIB: Geostatistical Software Library and Users Guide. Oxford Univ. Press, New York, p. 369.

Guerrero-Martínez, F.J., Prol-Ledesma, R.M., Carrillo-de la Cruz, J.L., Rodríguez-Díaz, A. A., Gonsáles-Romo, I.A., 2020. A Three-Dimensional Temperature Model of the Acoculco caldera complex, Puebla, Mexico, from the Curie isotherm as a Boundary Condition, 86. Geothermics, 101794. https://doi.org/10.1016/j.geothermics.2019.101794.

Kumar, R., Bansal, A.R., Ghods, A., 2020. Estimation of depth to bottom of magnetic sources using spectral methods: application on Iran's aeromagnetic data. J. Geophys. Res. Solid Earth 125, e2019JB018119. https://doi.org/10.1029/2019JB018119.

Li, C.-F., Shi, X., Zhou, Z., Li, J., Geng, J., Chen, B., 2010. Depths to the magnetic layer bottom in the South China Sea area and their tectonic implications. Geophys. J. Int. 182 (3), 1229–1247. https://doi.org/10.1111/j.1365-246X.2010.04702.x.

Li, C.-.F., Wang, J., Lin, J., Wang, T., 2013. Thermal evolution of the North Atlantic lithosphere: new constraints from magnetic anomaly inversion with a fractal magnetization model. Geochem. Geophys. Geosyst. 14 (12), 5078–5105. https://doi.org/10.1002/2013GC004896.

Manea, M., Manea, V.C., 2011. Curie point depth estimates and correlation with subduction in Mexico. Pure Appl. Geophys. 168, 1489–1499. https://doi.org/10.1007/s00024-010-0238-2.

Martos, Y.M., Catalán, M., Jordan, T.A., Golynsky, A., Golynsky, D., Eagles, G., Vaughan, D.G.D.G., 2017. Heat flux distribution of antarctica unveiled. Geophys. Res. Lett. 44 (22), 11417–11426. https://doi.org/10.1002/2017GL075609.

North American Magnetic Anomaly Group (NAMAG), 2002. Digital Data Grids for the Magnetic Anomaly Map of North America. U.S. Geol. Surv. Open File Rep, pp. 02–414. https://mrdata.usgs.gov/magnetic/.

Okubo, Y., Tsu, H., Ogawa, K., 1989. Estimation of Curie point temperature and geothermal structure of island arcs of Japan. Tectonophysics 159, 279–290.

Padilla y Sánchez, R.J., Domínguez Trejo, I., López Azcárraga, A.G., Mota Nieto, J., Fuentes Menes, A.O., Rosique Naranjo, F., Germán Castelán, E.A., Campos Arriola, S. E., 2013. National Autonomous University of Mexico Tectonic Map of Mexico GIS Project. American Association of Petroleum Geologists GIS Open Files series.

Prol-Ledesma, R.M., Arango-Galván, C., Torres-Vera, M.A., 2016. Rigorous analysis of available data from cerro prieto and las tres virgenes geothermal fields with calculations for expanded electricity generation. Nat Resour Res 25, 445–458. https://doi.org/10.1007/s11053-016-9295-2.

Prol-Ledesma, R.M., Carrillo-de la Cruz, J.L., Torres-Vera, M.A., Membrillo-Abad, A.S., Espinosa-Ojeda, O.M., 2018. Heat flow map and geothermal resources in Mexico. Terra Digitalis 2 (2), 1–15. https://doi.org/10.22201/igg.25940694.2018.2.51.

Pyrcz, M.J., Deutsch, C.V., 2014. Geostatistical Reservoir Modeling, 2nd Ed. Oxford University Press, New York.

Ravat, D., Pignatelli, A., Nicolosi, I., Champpini, M., 2007. A study of spectral methods of estimating the depth to the bottom of magnetic sources from near surface magnetic anomaly data. Geophys. J. Int. 169 (2), 421–434. https://doi.org/10.1111/j.1365-246X.2007.03305.x.

Ross, H.E., Blakely, R.J., Zoback, M.D., 2006. Testing the use of aeromagnetic data for the determination of Curie depth in California. Geophysics 71 (5), L51–L59. https://doi.org/10.1190/1.2335572.

Salem, A., Green, C., Ravat, D., Singh, K.H., East, P., Fairhead, J.D., Mogren, S., Biegert, E., 2014. Depth to Curie temperature across the central Red Sea from magnetic data using the de-fractal method. Tectonophysics 75–86. https://doi.org/10.1016/j.tecto.2014.04.027, 624–625.

Smith, D.L., Nuckels III, C.E., Jones, R.L., Cook, G.A., 1979. Distribution of heat flow and radioactive heat generation in northern Mexico. J. Geophys. Res. 84 (B5), 2371–2379. https://doi.org/10.1029/JB084iB05p02371.

SMU Node of national geothermal data system heat flow observation in content model format. http://geothermal.smu.edu/static/DownloadFilesButtonPage.htm. Accessed on February 25, 2020.

Tanaka, A., Okubo, Y., Matsubayashi, O., 1999. Curie point depth based on spectrum analysis of the magnetic anomaly data in East and Southeast Asia. Tectonophysics 306 (3–4), 461–470. https://doi.org/10.1016/S0040-1951(99)00072-4.

Turcotte, D.L., Schubert, G., 2002. Geodynamics. Cambridge University Press, p. 863.

Wang, J., Li, C.-.F., 2015. Crustal magmatism and lithospheric geothermal state of the western North America and their implications for magnetic mantle. Tectonophysics 638, 112–125. https://doi.org/10.1016/j.tecto.2014.11.002.

Wang, Y., Forsyth, D.W., Rau, C.J., Carriero, N., Schmandt, B., Gaherty, J.B., Savage, B., 2013. Fossil slabs attached to unsubducted fragments of the Farallon plate. Proc. Nat. Acad. Sci. 110, 5342–5346.